Optical Materials 167 (2025) 117290

Contents lists available at ScienceDirect

Optical Materials

journal homepage: www.elsevier.com/locate/optmat

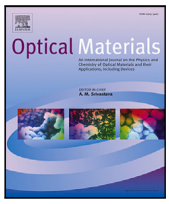

Research Article

Infrared dielectric function of photochromic thiazolothiazole-embedded polymer

Nuren Z. Shuchi [a,*], Tyler J. Adams [b], Naz F. Tumpa [b], Dustin Louisos [a], Glenn D. Boreman [a], Michael G. Walter [b], Tino Hofmann [c]

[a] Department of Physics and Optical Science, University of North Carolina at Charlotte, 9201 University City Blvd, Charlotte, 28223, NC, USA
[b] Department of Chemistry, University of North Carolina at Charlotte, 9201 University City Blvd, Charlotte, 28223, NC, USA
[c] Department of Physics, New Jersey Institute of Technology, University Heights, Newark, 07102, NJ, USA

ARTICLE INFO

Keywords:
Infrared dielectric function
Photochromic polymer
Spectroscopic ellipsometry
Thiazolothiazole

ABSTRACT

Optical technologies that offer dynamic spectral control have been becoming more prevalent in recent years. Driven by this increased demand for tunable optical devices, substantial research efforts have been dedicated to the development of novel photo-responsive materials. In recent years, photochromic thiazolo[5,4-d]thiazole (TTz)-embedded polymers has emerged as promising candidate for technologies ranging from optical recording systems, tunable metasurfaces, to tinted lenses and smart windows. To effectively design, fabricate, and optimize tunable optical devices incorporating photochromic thiazolothiazole-embedded polymers, an accurate understanding of their complex dielectric function is fundamental to contemporary research. In this work, the infrared dielectric function of photochromic dipyridinium thiazolo[5,4-d]thiazole embedded in polymer is reported. Bulk TTz-embedded polymer samples were prepared by drop casting and dehydration in room temperature. The samples were investigated using spectroscopic ellipsometry in the infrared spectral range from 500 cm^{-1} to 1800 cm^{-1} before and after photochromism induced by a 405 nm diode laser. The model dielectric functions of the thiazolothiazole-embedded polymer film for its TTz^{2+} (unirradiated) and TTz^{0} (irradiated) states are composed of a series of Lorentz oscillators in the measured spectral range. A comparison of the obtained complex dielectric functions for the TTz^{2+} and TTz^{0} states shows that the oscillators located in the spectral ranges 500 cm^{-1}–700 cm^{-1}, 1300 cm^{-1}–1400 cm^{-1}, and 1500 cm^{-1}–1700 cm^{-1} change in both amplitude and resonant frequency upon transition between the states. Additionally, a resonance at approximately 1050 cm^{-1} exhibited a change in oscillator amplitude but not resonant frequency due to the photochromic transition.

1. Introduction

Photochromism refers to the reversible transformation of a material between two states with distinct light absorption properties in different spectral regions induced by electromagnetic radiation [1]. Organic and inorganic photochromic materials have gained significant attention in recent years because of their potential applications in diverse fields. These applications include tinted lenses and smart windows, memory devices, actuators, tunable filters, and holographic gratings [2–5]. Organic photochromic materials are emerging as more promising candidates compared to their inorganic counterparts such as metal halides [6] and transition metal oxides [7] for applications demanding spectral tunability, lower processing cost, and mechanical flexibility [8].

Viologens constitute a significant class of organic photochromic materials [9]. The photochromic behavior of viologens arises from photoinduced electron transfer. This transfer occurs in an electron source, like polyvinyl alcohol/borax (PVA/borax) polymer matrix (molecular structure shown in Fig. 1(c)) to the pyridinium cation, resulting in the reduction of the pyridinium unit and the formation of a radical cation [10]. The polarity of the PVA/borax system contributes to its water solubility and makes it suitable for processing into low-toxicity, low-cost films. The alcohol groups in PVA enable crosslinking with borax, which lowers the oxidation potential, facilitating photo-oxidation by the viologen [11].

Viologens can be extended with a thiazolo[5,4-d]thiazole (TTz) fused, conjugated bridge. The rigid, planar backbone and extended π-conjugation of TTz-core contributes to its suitability in developing high-efficiency photochromic materials. This approach has been attracting

* Corresponding author.
E-mail address: nshuchi@charlotte.edu (N.Z. Shuchi).

https://doi.org/10.1016/j.optmat.2025.117290
Received 31 March 2025; Received in revised form 18 June 2025; Accepted 1 July 2025
Available online 13 July 2025

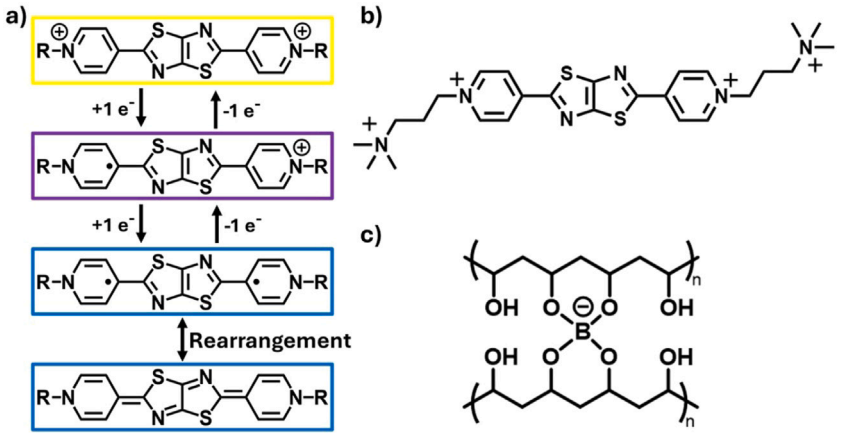

Fig. 1. (a) Two single electron reductions of dipyridinium TTz [12], (b) structure of $(NPr)_2TTz^{4+}$, (c) PVA/borax polymer matrix structure.

increasing interest as the resulting compound has strong fluorescence, solution-processability, and undergoes reversible photochromic transitions. In particular, dipyridinium thiazolo[5,4-d]thiazole viologens exhibit high-contrast, fast, and reversible photochromic changes when embedded in a polymer matrix.

N,N'-di(trimethylaminopropyl)-2,5-Bis(4-pyridinium)thiazolo[5,4-d] thiazole tetrabromide ($(NPr)_2TTz^{4+}$), shown in Fig. 1(b), a highly water-soluble derivative of dipyridinium TTz's, has been previously established as having high-contrast photochromism in the visible and near-infrared spectrum [11,12]. When exposed to radiation with an energy larger than 2.8 eV, it transitions from light yellow (TTz^{2+}) to purple ($TTz^{\cdot+}$) to blue (TTz^0) state due to two distinct photoinduced single electron reductions, as illustrated in Fig. 1(a). The reverse color change (to yellow/colorless) is driven by reaction of the TTz^0 state with molecular oxygen [11].

The accurate knowledge of the dielectric function is essential to contemporary research on the design, fabrication and optimization of tunable optical devices utilizing photochromic thiazolothiazole-embedded polymers. In particular finite element numerical calculations rely on dielectric function data for the simulation of complex structures and devices. We have previously addressed this knowledge gap and reported on the complex dielectric function of a nonphotochromic TTz derivative and a photochromic TTz-embedded polymer in the visible and near-infrared spectral range [11,13]. The infrared spectral range, however, has not yet been investigated.

In this paper, the first quantitative analysis of the complex infrared optical dielectric function of a photochromic thiazolo[5,4-d]thiazole-embedded polymer using spectroscopic ellipsometry is reported. Spectroscopic ellipsometry is the preeminent technology for the accurate determination of dielectric material responses. However, while spectroscopic ellipsometry has been used in the visible spectral range to investigate a wide range of photochromic materials, the direct ellipsometric investigation of photochromic materials in the infrared spectral range has been lacking [14]. In contrast to infrared reflection or transmission measurements which are frequently employed to investigate the infrared optical properties of photochromic polymers, our approach ensures the Kramers–Kronig consistency of the dielectric function.

A parameterized dielectric function of photochromic $(NPr)_2TTz^{4+}$ embedded in a polymer matrix was obtained through quantitative analysis of the polarization-sensitive optical response. The measurements were taken in the infrared spectral range from 500 cm^{-1} to 1800 cm^{-1} before and after irradiation with a 405 nm diode laser as an excitation source. The model dielectric functions of the thiazolothiazole-embedded polymer film for its TTz^{2+} (unirradiated) and TTz^0 (irradiated) states are composed of a series of Lorentz oscillators in the measured spectral range. A comparison of the obtained complex dielectric functions for the TTz^{2+} and TTz^0 state shows several infrared absorption bands for which both amplitude and resonant frequency change upon transition between the states. In addition, a resonance has been identified at approximately 1050 cm^{-1}, for which, only a change of the oscillator amplitude was observed due to the photochromic transition.

In addition to providing the infrared dielectric function for thiazolothiazole-embedded polymer in the oxidized and reduced state, the parameterized dielectric function of PVA/borax is reported. This provides a comparison between the thiazolothiazole-embedded polymer and the PVA/borax host-polymer.

2. Experiment

2.1. Synthesis and sample preparation

Dithiooxamide (1.9916 g, 16.6 mmol) and 4-pyridinecarboxaldehyde (4.4 mL, 46.7 mmol) were refluxed in 60 mL of dimethylformamide (DMF) at 153 °C for 8 h. The reaction mixture was cooled to room temperature, and the resulting tan precipitate was collected by vacuum filtration. The solid was washed with water and dried under vacuum to yield a tan solid (3.732 g, 75.9% yield). Molecular characterization data quantitatively matched previously reported values [11,12,15,16]. ^{1}H NMR (500 MHz, $CDCl_3$): 8.78 (dd, J = 1.6, 4.6 Hz, 4H), 7.88 (dd, J = 1.6, 4.6 Hz, 4H) ppm. MS (MALDI-TOF): m/z calculated for $C_{14}H_8N_4S_2$ = 296.376, found 298.66.

Py_2TTz (2.9906 g, 10.1 mmol) was heated with (3-bromopropyl)trimethylammonium bromide (6.5995 g, 25.3 mmol) in 35 mL of DMF under a nitrogen atmosphere at 100 °C for 72 h to alkylate the pyridine rings and increase its water solubility. The resulting yellow precipitate of N,N'-di(trimethylaminopropyl)-2,5-bis(4-pyridinium)thiazolo[5,4-d] thiazole ($(NPr)_2TTz^{4+}$) was collected by vacuum filtration, washed with DMF and acetonitrile, and dried in a vacuum oven to yield a yellow solid (7.2742 g, 87.8% yield). Molecular characterization data matched previously reported values [11,12,15]. ^{1}H NMR (500 MHz, D_2O): 2.55 (m, 4H), 3.08 (s, 18H), 3.46 (t, J = 8.0 Hz, 4H), 4.67 (t, J = 6.5 Hz, 4H), 8.59 (d, J = 5.5 Hz, 4H), 8.95 (d, J = 5.5 Hz, 4H) ppm.

Following the synthesis 3.4 wt% dipyridinium TTz was dissolved in polyvinyl alcohol solution and then borax is added into the mixture to obtain a TTz embedded polymer hydrogel as previously reported [12]. Bulk samples with a thickness of approximately 150 μ m were prepared by drop casting and dehydration at room temperature as illustrated in Fig. 2. In addition to the TTz embedded polymer sample, a reference sample composed of a polymeric system based on polyvinyl alcohol and borax (PVA/borax) without dipyridinium TTz was prepared using the same approach.

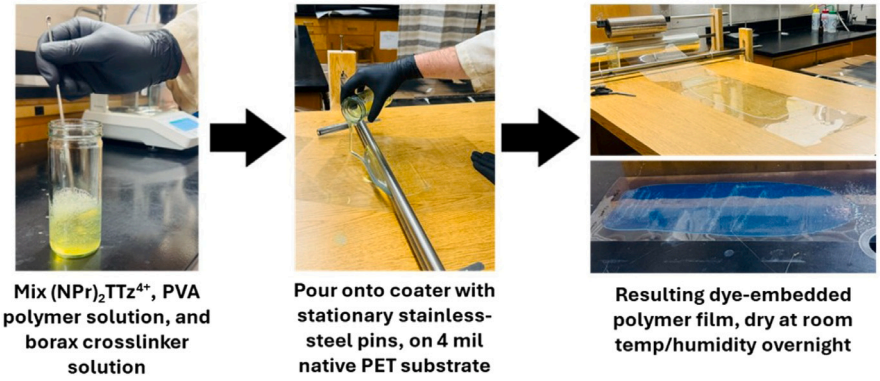

Fig. 2. Photographic images of the drop casting procedure. Following the synthesis and mixing with the PVA polymer and borax crosslinker solution, the mixture is poured onto a coater with a 4 mil native polyethylene terephthalate (PET) substrate. The resulting bulk sample is then dried at room temperature overnight.

2.2. Data acquisition and analysis

The reference and bulk TTz-embedded polymer samples were investigated using a commercial infrared ellipsometer (Mark I IR-VASE, J.A. Woollam Company). This ellipsometer operates in a rotating polarizer - sample - rotating compensator - rotating analyzer configuration as described in Ref. [17] and employs a Boman FTIR spectrometer and a DTGS detector. A 405 nm diode laser was used as an excitation source to investigate the optical properties of the TTz^0 state of the TTz-embedded polymer. The ellipsometric Ψ- and Δ-spectra were obtained before and after irradiation in the infrared spectral range from 500 cm^{-1} to 1800 cm^{-1} with a resolution of 8 cm^{-1} for a single angle of incidence Φ_a=65°. The incident angle was chosen due to its proximity to the Brewster angle. At the Brewster angle, the difference between the reflection coefficients of *s*- and *p*-polarized light is most pronounced. Since ellipsometry measures the amplitude ratio, Ψ and phase difference, Δ between these polarization states, measurements taken near the Brewster angle provide enhanced sensitivity to changes in optical properties. All measurements were carried out at room temperature in a nitrogen atmosphere. The nitrogen atmosphere prevents unintended transitions from the TTz^0 to the TTz^{2+} state due to oxidation during data acquisition.

The stratified optical layer calculations required for the analysis of the spectroscopic ellipsometry data were carried out using a commercial software package (WVASE32, J.A. Woollam Co. Inc.). For these calculations parameterized Kramers–Kronig consistent dispersion functions with sufficient flexibility to accurately reproduce the optical features of the experimental Ψ- and Δ-spectra (see Fig. 4) must be employed.

Sums of oscillators with Lorentzian broadening are widely used to describe the signatures of molecular or lattice vibrations in the infrared dielectric function [18]. This approach ensures that the extracted complex model dielectric function is Kramers–Kronig consistent. The use of parameterized dielectric function models offers an advantage over a point-by-point based analysis approach where ε_1 and ε_2 are determined independently for each wavelength. The former prevents experimental noise from entering the model dielectric function and ensures Kramers–Kronig consistency.

For the infrared model dielectric functions of both the reference sample and the TTz-embedded polymer in the TTz^{2+} and TTz^0 states it is found that a sum of oscillators with Lorentzian broadening describes the optical response well:

$$\varepsilon(E) = \varepsilon_1(E) + i\varepsilon_2(E) , \quad (1)$$
$$= \varepsilon_\infty + \sum_{k=1} \frac{A_k \gamma_k E_k}{E_k^2 - E^2 - i\gamma_k E} ,$$

where $\varepsilon_1(E)$ and $\varepsilon_2(E)$ are the real and imaginary parts of the complex dielectric function, respectively, as a function of the photon energy E. The relevant physical parameters A_k, E_k, and γ_k in the oscillator functions represent the oscillator amplitude, resonant energy, and broadening, respectively. The reference sample's dielectric function was adequately modeled with twelve Lorentz oscillators. The parameterized model dielectric function of the TTz-embedded polymer required eleven Lorentz oscillators to describe TTz^{2+} and TTz^0 states of the TTz-embedded polymer. Relevant parameters, such as oscillator amplitude, resonant energy, and broadening, were varied during the analysis using a Levenberg–Marquardt algorithm to minimize the weighted error function χ^2, and achieve the best fit between experimental and calculated data [19,20].

3. Results and discussion

Fig. 3 illustrates the experimental (dashed lines) and best-model calculated (red solid lines) Ψ-spectra (a) and Δ-spectra (b), respectively, for the TTz-embedded polymer in its TTz^{2+} (green dashed lines) in comparison to the PVA/borax reference sample (blue dashed lines). The experimental data were acquired at an angle of incidence Φ_a = 65° in a nitrogen environment. For visibility, the experimental and best-model calculated Ψ- and Δ-spectra for the PVA/borax reference sample are shown with an offset of 5° in Fig. 3. The similarity between the spectra for the PVA/borax reference sample and the TTz-embedded polymer in its TTz^{2+} state can be attributed to the moderate concentration of TTz (3.4 wt%) within the PVA/borax matrix. However, subtle differences in the ellipsometric data can be observed in the spectral regions of 1300–1400 cm^{-1} and 1500–1700 cm^{-1}. Especially, the absorption peaks observed in the PVA/borax reference at approximately 1327 cm^{-1} and 1562 cm^{-1} are suppressed in the spectra of the TTz-embedded polymer in its TTz^{2+} state. This suppression in the aforementioned spectral regions is associated with the presence of 3.4 wt% dipyridinium TTz in the polymer matrix.

Fig. 4 depicts the experimental (dashed lines) and best-model calculated (red solid lines) Ψ-spectra (a) and Δ-spectra (b), respectively, for the TTz-embedded polymer in its TTz^{2+} (green dashed lines) and TTz^0 states (blue dashed lines). For visibility, the experimental and best-model calculated Ψ- and Δ-spectra for the bulk TTz sample in the TTz^0 state are plotted with an offset of 5° in Fig. 4.

The experimental and best-model calculated Ψ- and Δ-spectra are in good agreement over the entire investigated spectral range in which a total of eleven vibration bands can be observed. The best-model fits yielded χ^2 values of 0.6075, and 0.6703 for the TTz^{2+} and TTz^0 states, respectively. These values indicate good agreement between the experimental and best-model calculated data over the measured spectral range [20].

Due to the moderate concentration of TTz within the PVA/borax matrix, the majority of the observed infrared absorption bands can be attributed to PVA/borax (see also Fig. 5). It is known that the

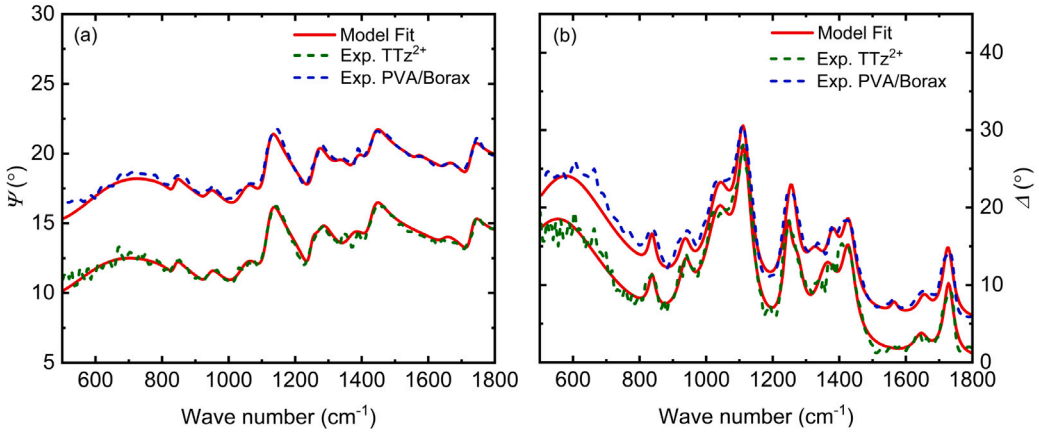

Fig. 3. Experimental (dashed lines) and best-model calculated (red solid lines) Ψ-spectra (a) and Δ-spectra (b), respectively, for the TTz^{2+} (green dashed lines) state of the bulk TTz-embedded polymer and the PVA/Borax reference sample (blue dashed lines). The spectra were obtained at a single angle of incidence $\Phi_a = 65°$ under nitrogen atmosphere at room temperature. The spectra for the PVA/Borax reference sample are depicted with an offset of 5° for visibility.

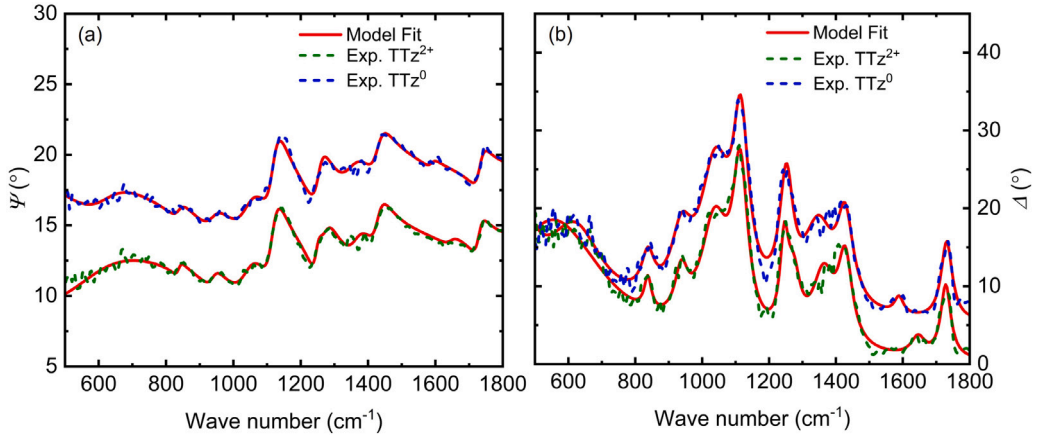

Fig. 4. Experimental (dashed lines) and best-model calculated (red solid lines) Ψ-spectra (a) and Δ-spectra (b), respectively, for TTz^{2+} (green dashed lines) and TTz^0 (blue dashed lines) states of the bulk TTz-embedded polymer sample. These spectra were obtained at a single angle of incidence $\Phi_a = 65°$ under nitrogen atmosphere at room temperature. The spectra for TTz^0 state are depicted with an offset of 5° for visibility.

vibration bands observed at approximately 847 cm^{-1} and 1104 cm^{-1} can be attributed to the symmetric and asymmetric stretching vibrations of B_4–O, respectively [21–23]. Additional resonances are observed approximately at 1417 cm^{-1} and 1661 cm^{-1}. These resonances correspond to asymmetric stretching relaxation of B–O–C and the bending vibration of HOH in water molecules, respectively [23].

In contrast to vibrational bands attributed to PVA/borax, the photochromically-induced, infrared-optical changes to the TTz viologen can be observed only as very subtle features. The most prominent photochromic changes can be noticed at approximately 1600 cm^{-1} and below 750 cm^{-1}. Additional photochromic changes occur at approximately 1050 cm^{-1} and between 1300 and 1400 cm^{-1}.

As discussed above, the majority of the observed infrared absorption bands can be attributed to PVA/borax. This is corroborated by a direct comparison of the ellipsometric data of the PVA/borax reference sample to the TTz-embedded polymer sample as shown in Fig. 3.

Figs. 5(a) and 5(b) show the real ε_1 and imaginary ε_2 components of the best-fit parameterized model dielectric functions for the reference sample, and the TTz-embedded polymer sample in the TTz^{2+}, and TTz^0 states. Shaded regions in these figures highlight the spectral regions where the dielectric function of the TTz-embedded polymer before and after irradiation with a 405 nm diode laser and dielectric function of the reference sample deviate from each other.

In the following section, we will focus primarily on the imaginary part of the dielectric function to discuss the observed infrared absorption bands. As can be seen in Fig. 5(b) the main infrared absorption bands are due to PVA/Borax (red solid lines). These bands include the symmetric and asymmetric stretching vibrations of B_4–O, asymmetric stretching relaxation of B–O–C and the bending vibration of HOH in water molecules [21–23].

The imaginary part ε_2 of infrared dielectric function of the reference sample, within the measured spectral range, exhibits several prominent absorption peaks as shown in Fig. 5(b). The dielectric response for the TTz^{2+} state of the TTz-embedded polymer closely resembles the absorption features of the reference sample. This similarity in optical response is a consequence of the low concentration of dipyridinium TTz incorporated into the cross-linked PVA/borax polymer. However, distinct spectral differences are also evident in Fig. 5(b). Notably, in the spectra of the TTz-embedded polymer in its TTz^{2+} state, the absorption peaks seen in the PVA/borax reference at approximately 1327 cm^{-1} and 1562 cm^{-1} are suppressed. This suppression in the 1300–1400 cm^{-1} and 1500–1700 cm^{-1} spectral regions is attributed to the presence of 3.4 wt% dipyridinium TTz in the polymer matrix. Furthermore, a comparison of the complex dielectric functions obtained for the TTz-embedded polymer before and after irradiation reveals that oscillators in the spectral ranges of 500–700 cm^{-1}, 1300–1400 cm^{-1}, and 1500–1700 cm^{-1} exhibit changes in both amplitude and resonant frequency upon transition between these states. Additionally, a resonance near 1050 cm^{-1} was identified, where only an amplitude change was observed due to the photochromic transition.

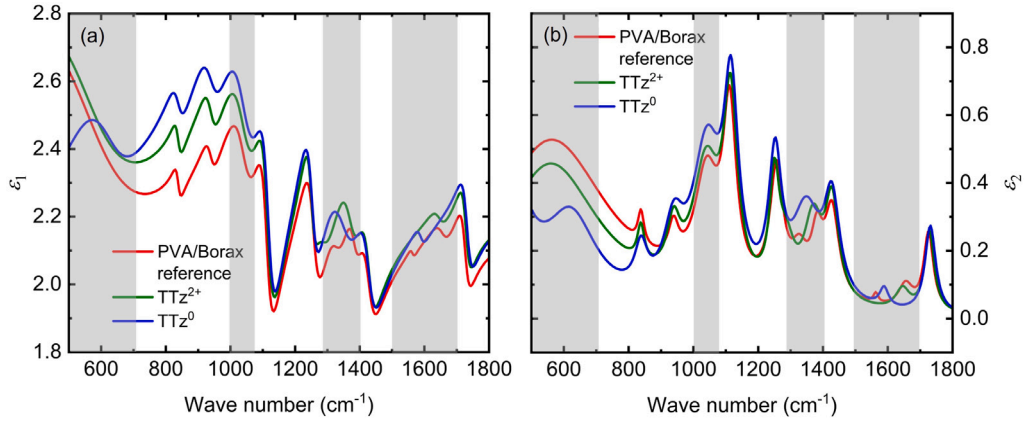

Fig. 5. Comparison between the real ε_1 (a) and imaginary ε_2 parts (b) of the best-fit parameterized model dielectric functions for PVA/Borax (red solid lines), TTz^{2+} (green solid lines), and TTz^0 (blue solid lines) states. The shaded regions illustrate the spectral windows where photochromically induced changes in the infrared dielectric function of the TTz-embedded polymer occur.

4. Conclusion

In conclusion, the fabricated bulk TTz-embedded polymer samples were studied before and after irradiation with a 405 nm diode laser in the spectral range from 500 cm^{-1} to 1800 cm^{-1}. To describe the optical features of the TTz-embedded polymer accurately, complex-valued model dielectric functions composed of Lorentz oscillators were used for both states. A comparative study of the obtained complex dielectric functions for the TTz^{2+} and TTz^0 states reveals that the oscillators located in the spectral ranges 500 cm^{-1}–700 cm^{-1}, 1300 cm^{-1}–1400 cm^{-1}, and 1500 cm^{-1}–1700 cm^{-1} change in both amplitude and resonant frequency upon transition between the states. Furthermore, after the photochromic transition, the resonance near 1050 cm^{-1} exhibited a change in amplitude but not in resonant frequency. By providing a detailed analysis of the TTz polymer's optical transitions in the spectral range from 500 cm^{-1} to 1800 cm^{-1} before and after irradiation, the work reported here establishes a foundation for integrating TTz-based materials into infrared-tunable optical devices.

CRediT authorship contribution statement

Nuren Z. Shuchi: Writing – review & editing, Writing – original draft, Methodology, Investigation, Formal analysis, Data curation, Conceptualization. **Tyler J. Adams:** Writing – review & editing, Methodology, Investigation. **Naz F. Tumpa:** Writing – review & editing, Methodology, Investigation. **Dustin Louisos:** Writing – review & editing, Investigation, Formal analysis. **Glenn D. Boreman:** Writing – review & editing, Resources, Project administration. **Michael G. Walter:** Writing – review & editing, Validation, Supervision, Resources, Investigation. **Tino Hofmann:** Writing – review & editing, Validation, Supervision, Project administration, Funding acquisition, Conceptualization.

Funding

The authors acknowledge the support from the National Science Foundation within the IUCRC Center for Metamaterials, United States (2052745) and National Science Foundation, United States Grant (CHE-2400165).

Declaration of competing interest

The authors declare that they have no known competing financial interests or personal relationships that could have appeared to influence the work reported in this paper.

Acknowledgments

The authors would like to acknowledge the support from the Department of Physics and Optical Science and the Department of Chemistry at the University of North Carolina at Charlotte. We further acknowledge support from the Center for Optoelectronics and Optical Communications, the Division of Research, and the Klein College of Science at UNC Charlotte.

Data availability

Data will be made available on request.

References

[1] J. Crano, R.J. Guglielmetti, Organic Photochromic and Thermochromic Compounds Volume 1: Main Photochromic Families, vol. 1, Kluwer Academic Publishers. 10, New york, NY, 1999, p. b115590.
[2] A.M. Österholm, D.E. Shen, J.A. Kerszulis, R.H. Bulloch, M. Kuepfert, A.L. Dyer, J.R. Reynolds, Four shades of brown: tuning of electrochromic polymer blends toward high-contrast eyewear, ACS Appl. Mater. Inter. 7 (3) (2015) 1413–1421.
[3] H. Cho, E. Kim, Highly fluorescent and photochromic diarylethene oligomer bridged by p-phenylenevinylene, Macromolecules 35 (23) (2002) 8684–8687.
[4] T. Ikeda, J.-i. Mamiya, Y. Yu, Photomechanics of liquid-crystalline elastomers and other polymers, Angew. Chem. Int. Ed. 46 (4) (2007) 506–528.
[5] C. Bertarelli, A. Bianco, R. Castagna, G. Pariani, Photochromism into optics: Opportunities to develop light-triggered optical elements, J. Photochem. Photobiol. C 12 (2) (2011) 106–125.
[6] X.-X. Li, S.-T. Zheng, Three-dimensional metal-halide open frameworks, Coord. Chem. Rev. 430 (2021) 213663.
[7] W. Meng, A.J. Kragt, Y. Gao, E. Brembilla, X. Hu, J.S. van der Burgt, A.P. Schenning, T. Klein, G. Zhou, E.R. van den Ham, et al., Scalable photochromic film for solar heat and daylight management, Adv. Mater. 36 (5) (2024) 2304910.
[8] J. Clark, G. Lanzani, Organic photonics for communications, Nat. Phot. 4 (7) (2010) 438–446.
[9] Z. Guo, Y. Su, H. Zong, F. Zhou, M. Wang, G. Zhou, A universal strategy for reversible photochromism of viologen derivatives in solutions, Adv. Opt. Mater. 12 (2024) 2401791.
[10] J. Peon, X. Tan, J.D. Hoerner, C. Xia, Y.F. Luk, B. Kohler, Excited state dynamics of methyl viologen. ultrafast photoreduction in methanol and fluorescence in acetonitrile, J. Phys. Chem. A 105 (24) (2001) 5768–5777.
[11] T.J. Adams, N.F. Tumpa, M. Acharya, Q.H. Nguyen, N. Shuchi, M. Baliukonis, S.E. Starnes, T. Hofmann, M.G. Walter, Achieving smart photochromics using water-processable, high-contrast, oxygen-sensing, and photoactuating thiazolothiazole-embedded polymer films, ACS Appl. Opt. Mater. 2 (5) (2024) 704–713.
[12] T.J. Adams, A.R. Brotherton, J.A. Molai, N. Parmar, J.R. Palmer, K.A. Sandor, M.G. Walter, Obtaining reversible, high contrast electrochromism, electrofluorochromism, and photochromism in an aqueous hydrogel device using chromogenic thiazolothiazoles, Adv. Funct. Mater. 31 (36) (2021) 2103408.

[13] N. Shuchi, J. Mower, V.P. Stinson, M.J. McLamb, G.D. Boreman, M.G. Walter, T. Hofmann, Complex dielectric function of thiazolothiazole thin films determined by spectroscopic ellipsometry, Opt. Mat. Exp. 13 (6) (2023) 1589–1595.
[14] Y.-G. Mo, R. Dillon, P. Snyder, Spectroscopic analysis of photochromic films, J. Vac. Sci. Technol. A 17 (1) (1999) 170–175.
[15] J. Luo, B. Hu, C. Debruler, T.L. Liu, A π-conjugation extended viologen as a two-electron storage anolyte for total organic aqueous redox flow batteries, Angew. Chem. 130 (1) (2018) 237–241.
[16] A.N. Woodward, J.M. Kolesar, S.R. Hall, N.-A. Saleh, D.S. Jones, M.G. Walter, Thiazolothiazole fluorophores exhibiting strong fluorescence and viologen-like reversible electrochromism, J. Am. Chem. Soc. 139 (25) (2017) 8467–8473.
[17] H. Fujiwara, Spectroscopic Ellipsometry: Principles and Applications, John Wiley & Sons, 2007.
[18] R. Synowicki, T.E. Tiwald, Optical properties of bulk c-ZrO_2, c-MgO and a-As_2S_3 determined by variable angle spectroscopic ellipsometry, Thin Solid Films 455 (2004) 248–255.
[19] G. Jellison Jr., V. Merkulov, A. Puretzky, D. Geohegan, G. Eres, D. Lowndes, J. Caughman, Characterization of thin-film amorphous semiconductors using spectroscopic ellipsometry, Thin Solid Films 377 (2000) 68–73.
[20] G.E. Jellison Jr., Data analysis for spectroscopic ellipsometry, Thin Solid Films 234 (1–2) (1993) 416–422.
[21] A.A.R.d. Oliveira, V.S. Gomide, M.d.F. Leite, H.S. Mansur, M.d.M. Pereira, Effect of polyvinyl alcohol content and after synthesis neutralization on structure, mechanical properties and cytotoxicity of sol–gel derived hybrid foams, Mater. Res. 12 (2009) 239–244.
[22] H.K. Dave, K. Nath, Synthesis, characterization and application of disodium tetraborate cross-linked polyvinyl alcohol membranes for pervaporation dehydration of ethylene glycol., Acta. Chim. Slov. 65 (4) (2018).
[23] M.B. Lawrence, Influence of cross-linker concentration on the water contained within the pores of poly (vinyl alcohol)-borax hydrogels: a vibrational spectroscopic study, Polym. Bull. 81 (2024) 13783–13801.